Journal of Marine Research, 54, 1017–1037, 1996

The principle of biological attraction, demonstrated by the bio-continuum theory of zooplankton patch dynamics

by Meng Zhou[1] and Mark E. Huntley[1]

ABSTRACT

A theory of zooplankton and micronekton patch dynamics is developed that expressly includes animal behavior. This represents a departure from traditional models of patch dynamics, which generally treat animals as Lagrangian particles whose distributions are determined solely by processes of advection and diffusion. The "bio-continuum" theory is based on principles of statistical mechanics, and describes animal aggregations in terms of mean motion, random motion, random kinetic energy, distribution and abundance. The forces on an animal aggregation act both upon the aggregation as a whole (external forces) or between individuals (internal forces). We demonstrate here that the internal forces which serve to maintain autocoherence are, in essence, a force of biological attraction that can be quantified in Newtons. A coefficient of biological attraction is defined, and its magnitude evaluated in aggregations of Antarctic euphausiids (*Euphausia superba*). We hypothesize that the coefficient of biological attraction may be constant for all organisms in the sea.

A method for measuring all key variables with acoustic Doppler technology is presented, with specific attention to application of the Acoustic Doppler Current Profiler (ADCP). We conclude that bio-continuum theory, coupled with acoustic Doppler observations, provides a practical approach for studying animal aggregation dynamics in the sea.

1. Introduction

Patchiness of zooplankton and micronekton is an important feature of the ocean. It has been well recognized in many individual species, and is critical in determining the fate of natural populations in a dynamic physical environment. Early studies of patch dynamics emphasized the role of intraspecific autocoherence on patch size (Anderson, 1981; Okubo, 1980; Parr, 1927). A typical model by Anderson (1981) describes the size of a fish school as being governed by Fokker-Planck stochastic differential equations. Dynamics were introduced into models of patchiness by Okubo and Anderson (1984) and Okubo (1986). In their theory, the equation of motion is Newtonian, so that the acceleration of an animal is determined by the friction force, autocoherence, and a random Markovian acceleration. From these assumptions, A Fokker-Planck equation was used to describe the probability-density function. Under equilibrium conditions, the velocity distribution is Maxwellian and fits observed data of an insect swarm very well. However, behavior, per se, did not enter

1. Scripps Institution of Oceanography, La Jolla, California 92093-0202, USA.

into consideration. Similarly, Steele and Henderson's (1992) model of plankton patchiness uses white-noise forcing of a simple phytoplankton-zooplankton Lotka-Volterra model, with diffusion, to produce power spectra of wave-number variance that match observations. The results, in both cases, resemble real situations in terms of statistical means of integral scales, but provide little insight into the animal behaviors that are one of the prime underlying causes of patchy distributions.

Recent attempts to resolve this dilemma have been only partially fruitful. Models consisting of *n*-individual animal models have been developed to understand the random movement of animals in a swarm or a school, and the resulting density distribution (Okubo, 1986). Unfortunately, the ability of such *n*-individual models to reproduce the dynamics of a patch is restricted by our knowledge of individual behavior and by an existing computing power.

Behavior clearly plays a role in patch dynamics. Aggregative behavior confers advantages in avoiding predation (Brock and Riffenburgh, 1960; Clark, 1974; Partridge, 1982; Pitcher, 1983; Swartzmann, 1991) and in utilizing food resources that are themselves patchily distributed (Cowles *et al.,* 1993; Duffy and Wissel, 1988). Therefore, animals are not simply passive particles that respond stochastically to processes of advection and diffusion. They actively aggregate near food sources, they swim to avoid predators, and they move to desired locations or environments (e.g. Blaxter, 1969; Radakov, 1973; Shaw, 1978). These behaviors are the mechanisms that maintain the autocoherence of aggregations.

Advection-diffusion equations cannot describe behavioral processes that determine patch dynamics. This raises two important questions. First, what system of equations can explain how animals respond to environmental forces such as food sources, predators, light, and flow fields? Second, what mechanics determine the distribution and swimming velocities of individuals, their attraction to one another, and the shape of their aggregations? A theory of patch dynamics should incorporate these aspects, building on what we know about physical laws of motion and the behavioral responses of animals to their environment.

The ability to observe patches of zooplankton and micronekton has greatly improved in the past decade through the use of bioacoustic methods (e.g. Smith *et al.,* 1992). We draw particular attention to the use of acoustic Doppler technology. Like all bioacoustic methods, this approach provides observations of distribution and abundance (Flagg and Smith, 1989; RDI, 1989; Zhou *et al.,* 1994). However, Doppler spectra can also be used to make direct measurements of animal swimming speeds, as was first shown by Holliday's (1974; 1977) measurements on fish. This unique feature, as well as the widespread use of one particular instrument, the Acoustic Doppler Current Profiler (ADCP), provides an opportunity to bridge the gap between observations and an improved theory of patch dynamics. Measurements of animal mean motion and random motion are precisely what is required to measure those aspects of animal behavior lacking in current models of plankton and nekton patch dynamics.

The theory developed in this article specifically parameterizes animal behavior. Dividing an animal's motion into its mean and random components, and applying Boltzmann's transport equation leads us to derive equations of motion that govern patch dynamics, acknowledging fundamental laws of physics that go beyond the recognition of simple advective and diffusive processes. The resulting dynamical theory describes animal swarms in terms of measurable macro-phenomena (e.g. animal abundance, mean velocities, and random motion), which constitute what we refer to as the "bio-continuum." A special feature of the theory is that these macrovariables can be measured by acoustic Doppler techniques.

2. Basic theory

An animal's motion may be determined by complicated processes of physiology and behavior; nevertheless, it is an adequate assumption that the motion of the animal is governed by Newton's second law (Okubo, 1986; Okubo and Anderson, 1984), i.e.

$$\frac{d\mathbf{x}}{dt} = \mathbf{v} \tag{1}$$

and

$$\frac{d\mathbf{v}}{dt} = \mathbf{F}(\mathbf{x}, t) \tag{2}$$

where $\mathbf{x}$ is the vector describing the animal's position relative to the origin of the coordinate system, $\mathbf{v}$ is its velocity, and $\mathbf{F}$ is the ratio, to the animal's mass, of all forces acting on it. Noting that $f(\mathbf{x}, \mathbf{v}, t)$ is the distribution function of animals at time t at $\mathbf{x}$ with a velocity $\mathbf{v}$, we have the distribution function at $t + \Delta t$ as

$$f\left(\mathbf{x} + \mathbf{v}\Delta t, \mathbf{v} + \frac{d\mathbf{v}}{dt}\Delta t, t + \Delta t\right) = f(\mathbf{x}, \mathbf{v}, t) + (\Delta f)_C + (\Delta f)_B + (\Delta f)_P \tag{3}$$

where $(\Delta f)_C$ is the redistribution caused by "avoidance interactions" between animals. By this we refer to events in which two animals alter their velocities to avoid potential collisions, thus causing their redistribution. Such avoidance events are the mechanism by which individuals within patches are able to maintain relatively constant nearest neighbor distance (Test and McCann, 1976; Hamner *et al.*, 1989). The population dynamics term, $(\Delta f)_B$, describes the change due to processes of birth and mortality. The physiological term, $(\Delta f)_P$, refers to the change of velocities caused by physiological states of animals. Examples of such changes among marine zooplankton include diel variation in feeding activity (e.g. Baars and Oosterhuis, 1985; Dam and Peterson, 1993), which in turn affects physiological processes such as digestive metabolism (Head *et al.*, 1984; Mayzaud *et al.*, 1984), respiratory metabolism (Duval and Geen, 1976; Steele and Mullin, 1977), and is often accompanied by changes in swimming activity (Dagg, 1985; Huntley and Brooks,

1982; Saiz *et al.,* 1993). For example, the feeding activity of micronektonic *Euphausia superba* directly affects swimming behavior, causing "feeding frenzies" that involve turning, somersaulting and rapid swimming in the presence of high concentrations of food (Hamner, 1984; Stretch *et al.,* 1988).

Rearranging Eq. 3, and taking the limit as $\Delta t \rightarrow dt$, we obtain Boltzmann's transport equation as

$$\frac{\partial f}{\partial t} + \mathbf{v} \cdot \nabla_{\mathbf{x}} f + \mathbf{F}(\mathbf{x}, t) \cdot \nabla_{\mathbf{v}} f = \left(\frac{\partial f}{\partial t}\right)_C + \left(\frac{\partial f}{\partial t}\right)_B + \left(\frac{\partial f}{\partial t}\right)_P \tag{4}$$

where $\nabla_{\mathbf{x}}$ and $\nabla_{\mathbf{v}}$ are gradient operators corresponding to $\mathbf{x}$ and $\mathbf{v}$.

We now define the following variables in their standard forms (Degroot and Mazur, 1962):

$$\rho(\mathbf{x}, t) = \int_{-\infty}^{+\infty} f(\mathbf{x}, \mathbf{v}, t)\, dA_{\mathbf{v}} \qquad (\text{numbers m}^{-3}) \tag{5}$$

where ρ is animal abundance and $dA_{\mathbf{v}}$ is an infinitesimal volume in $\mathbf{v}$-space. The mean swimming velocity, $\mathbf{u}$, is given as

$$\mathbf{u}(\mathbf{x}, t) = \frac{1}{\rho} \int_{-\infty}^{+\infty} \mathbf{v} f(\mathbf{x}, \mathbf{v}, t)\, dA_{\mathbf{v}} \qquad (\text{m s}^{-1}) \tag{6}$$

We define a correlation tensor, Π,

$$\Pi(\mathbf{x}, t) = \int_{-\infty}^{+\infty} (\mathbf{v} - \mathbf{u})(\mathbf{v} - \mathbf{u}) f(\mathbf{x}, \mathbf{v}, t)\, dA_{\mathbf{v}} \qquad (\text{numbers m}^{-1}\ \text{s}^{-2}) \tag{7}$$

which describes the correlated motion between those components of velocity induced by avoidance between animals. Units of the correlation tensor, for an animal of unit mass (kg) are [N kg^{-1} m^{-2}], which are units of "pressure," i.e. a force acting on a unit surface, and we therefore refer to it simply as a pressure tensor. Thus, the tensor of Definition (7) also describes the rates of exchange of momentum between components of velocity due to the avoidance between animals. The random kinetic energy, θ, in unit volume of the aggregation is defined as

$$\theta(\mathbf{x}, t) = \frac{1}{2\rho} \int_{-\infty}^{+\infty} |\mathbf{v} - \mathbf{u}|^2 f(\mathbf{x}, \mathbf{v}, t)\, dA_{\mathbf{v}} \qquad (\text{m}^2\ \text{s}^{-2}) \tag{8}$$

and

$$J(\mathbf{x}, t) = \frac{1}{2} \int_{-\infty}^{+\infty} (\mathbf{v} - \mathbf{u}) |\mathbf{v} - \mathbf{u}|^2 f(\mathbf{x}, \mathbf{v}, t)\, dA_{\mathbf{v}} \qquad (\text{numbers s}^{-3}) \tag{9}$$

describes the correlation between the random motion component $(\mathbf{v} - \mathbf{u})$ and the kinetic energy component $[|\mathbf{v} - \mathbf{u}|^2]$, i.e. the flux of random kinetic energy across a boundary of volume $dA_{\mathbf{v}}$.

To simplify the problem, we follow standard procedures in statistical mechanics

(Degroot and Mazur, 1962). We make the following assumptions, that (1) momentum is conserved during avoidance events, and (2) only binary avoidance can occur.

Integrating Eq. 4 and substituting Definitions 5–9, we obtain the basic equations for the "bio-continuum" as

$$\frac{\partial \rho}{\partial t} + \nabla \cdot (\mathbf{u}\rho) = r_n(\text{birth, death}) \qquad \text{Continuity} \tag{10}$$

$$\frac{\partial \mathbf{u}}{\partial t} + \mathbf{u} \cdot \nabla \mathbf{u} + \frac{1}{\rho} \nabla \cdot \Pi = \frac{1}{\rho} \mathbf{F}_v \qquad \text{Momentum} \tag{11}$$

$$\frac{\partial \theta}{\partial t} + \mathbf{u} \cdot \nabla \theta + \frac{1}{\rho} \Pi : \nabla \mathbf{u} + \frac{1}{\rho} \nabla \cdot J = \frac{1}{\rho} Q_v \qquad \text{Internal energy.} \tag{12}$$

The conservation of numbers is described by Eq. (10), where r_n is the rate of change in animal abundance related to population dynamics. The momentum balance is described by Eq. (11), where $\mathbf{F}_v$ is the sum of all forces (in N kg^{-1} m^{-3}), both among animals (internal, or auto-coherence forces) and upon animals from their environment (external forces), acting on individuals in a unit volume. The third equation represents the conservation of random kinetic energy, where the rate of change of activity due to change in physiological state (Q_v) is balanced by the rate of change in random kinetic energy ($d\theta/dt$), the advection of random kinetic energy, ($\mathbf{u} \cdot \nabla\theta$), the interaction between random motion and nonuniform mean velocities [$(1/\rho)\Pi:\nabla\mathbf{u}$], and the flux of random kinetic energy [$(1/\rho)\nabla \cdot J$].

The above three formulations are the governing equations of motion in animal aggregations. The left side of each equation describes the mechanics which govern the motion; the right side represents biological phenomena, described in terms of population dynamics, behavior, and physiology. To close these equations requires further development of both the mechanical and biological aspects. First, we require closure of the constitutive functions for Π and J. Second, it is necessary to clearly parameterize the biological forces and suggest how they may be measured. In the following section, we discuss the constitutive functions and methods for their measurement.

3. Development of constitutive and state functions

a. Simplification of Π *and* J. If the random component of animal motion is isotropic within an aggregation, then Π is symmetric from Definition (7). We define a "normal pressure," p, as

$$p(\mathbf{x}, t) = \frac{1}{3} \int_{-\infty}^{+\infty} |\mathbf{v} - \mathbf{u}|^2 f(\mathbf{x}, \mathbf{v}, t)\, dA_{\mathbf{v}} \tag{13}$$

which describes, for avoiding animals, the correlation between those components of post-avoidance motion that are in the same direction as their original motion. We also

define a shear stress tensor, E, as

$$\mathrm{E} = \Pi - p\mathrm{I} \tag{14}$$

which describes the lateral redistribution of their motion due to such avoidance. The diagonal elements of E are equal to zero if the random motion is isotropic. From Definitions (8) and (13) we have the state function as

$$p = \tfrac{2}{3}\theta\rho \tag{15}$$

which represents the normal pressure as a function of random kinetic energy and the abundance of animals. From Definitions (9) and (14), E and J represent fluxes of momentum and random kinetic energy, respectively. The zero order approximation, from phenomenological theory (DeGroot and Mazur, 1962), is that the fluxes are proportional to the gradients of macrovariables, i.e.

$$\mathrm{E} = -\gamma\nabla\mathbf{u} \tag{16}$$

where γ is the momentum flux coefficient, and

$$J = \mu\nabla\theta \tag{17}$$

where μ is the random kinetic energy flux coefficient. We note that Eqs. (16) and (17) could be made more complicated as a function of velocities, random kinetic energy, abundance and time history. However, the simplifying assumptions we make here do not affect the general result. Given the simplifications of Eqs. (15)–(17), then Eqs. (10)–(12) and (14)–(17) provide a complete set of basic equations adequate to describe the dynamics of animal aggregations.

For the more complicated case of anisotropic random motion, such as might be encountered in a patch of Antarctic euphausiids, the horizontal motion of animals is stronger than their vertical motion (Hamner *et al.*, 1989). We note that Definition (7) can be expressed as

$$\Pi = \{p_{ij}\} \qquad (i, j = x, y, z)$$

where, for example, p_{xy} is the correlation between the x and y components of random motion velocity and, similarly,

$$\mathrm{E} = \{e_{ij}\} \qquad (i, j = x, y, z).$$

Thus, if $\epsilon = W/U$ is the ratio of the vertical to horizontal motion, where W and U are the scales of vertical and horizontal motion respectively, we have

$$p_{zz} = \epsilon p_{xx} = \epsilon p_{yy} \tag{18}$$

and

$$e_{ij} = \gamma_{ij}\frac{\partial u_i}{\partial x_j} \qquad i \neq j \tag{19}$$

where γ_{xz} is a symmetric tensor of momentum flux coefficients which satisfies $\gamma_{xz} = \gamma_{yz} = \epsilon\gamma_{xy}$. If we have $\epsilon \ll 1$, then we have $p_{xx} + p_{yy} + p_{zz} \approx p_{xx} + p_{yy}$, because $p_{zz} \to 0$. The normal pressure can then be expressed as $p = (p_{xx} + p_{yy})/2$. As a result, the state function becomes

$$p = \rho\theta. \tag{20}$$

b. The Bio-force, $\mathbf{F}_v$. In Eqs. (1) and (2) we have assumed that Newton's second law describes animal motion (Duffy and Wissel, 1988; Okubo, 1986; Okubo and Anderson, 1984); so, from Eq. (11)

$$\mathbf{F}_v = \rho(\mathbf{F}_E + \mathbf{F}_I) \tag{21}$$

where $\mathbf{F}_I$ is the internal force due to autocoherence in unit volume, and $\mathbf{F}_E$ is the sum of external biological forces, both acting on an individual of unit mass and having units of [N kg^{-1}]. The sum of these internal and external forces we term the "bio-force."

The external force, $\mathbf{F}_E$, can be parameterized with reference to food, temperature, predators, and other environmental influences. It is obvious that a complete and general parameterization would be complex, given the many variables known to affect animal behavior, and will not be attempted here. In this article we make the reasonable assumption that the effects of temperature, predators, light, and other environmental forces are, to a first order approximation, uniform within any aggregation of animals. These forces tend to act upon the aggregation as a whole.

The internal force, $\mathbf{F}_I$, is the sum of forces between individuals that act to maintain their association with one another. This is a force of autocoherence, and it is therefore a function of the distance between animals, their abundance, and species-specific recognition mechanisms. Because autocoherence acts between animals, its integration over the entire patch must be equal to zero. A simple linear form for the internal force is:

$$\mathbf{F}_I(\mathbf{x}, t) = \frac{c_g}{4\pi}\int_{-\infty}^{\infty}(\boldsymbol{\xi} - \mathbf{x})|\boldsymbol{\xi} - \mathbf{x}|^{-n}M\rho(\boldsymbol{\xi}, t)\, dA_{\boldsymbol{\xi}} \tag{22}$$

where $\boldsymbol{\xi}$ is position in the $\mathbf{x}$ domain, c_g is the autocoherence scale coefficient, M is individual body mass, and n is an exponent. The value of n arises from the mechanisms that animals use to communicate with one another, which determine their consequent motion. One hypothesis is that, with respect to one another, animals orient their motion according to "gradients of information," such as the concentration of chemical substances or acoustic signals (Bollens *et al.*, 1994; Buskey and Stoecker, 1989; Poulet and Ouellet, 1982). Such gradients are, in general, satisfied by the reverse quadratic law in three dimensional space and therefore diminish in intensity as the square of the distance from the source of the stimulus. Thus, n must be equal to 3. With $n = 3$, the autocoherent force, $\mathbf{F}_I(\mathbf{x}, t)$, has the

potential, $G(x)$, i.e.

$$G(\mathbf{x}) = -\frac{c_g}{4\pi|\mathbf{x}|} \tag{23}$$

and, substituting into (22), we obtain

$$\mathbf{F}_I(\mathbf{x}, t) = \nabla_{\mathbf{x}} \int_{-\infty}^{\infty} M\rho(\boldsymbol{\xi}, t)G(\boldsymbol{\xi} - \mathbf{x})\, dA_{\boldsymbol{\xi}}. \tag{24}$$

Formulae (22) and (23) will hold when the distance between animals is greater than r_e, referred to as the "equilibrium distance" (Parr, 1927; Breder, 1951; Okubo, 1986). The equilibrium distance is finite, and is generally greater than animal body length. In this article we focus on an analysis of the internal, autocoherent force, $\mathbf{F}_I$.

c. Equilibrium of random motion. One further assumption we make here is that the local adjustment of animal position is independent of mean distribution and motion. In other words, the time scale required for an animal to adjust its position relative to its neighbors is much smaller than the time scale of the mean motion of the aggregation. This is the local equilibrium assumption, i.e., that in a small volume, the random kinetic energy (θ), abundance (ρ) and pressure (p) are uniform, and therefore the effect of mean motion can be ignored.

The energy added to the total random energy of animals, δQ, in unit volume is divided into $\delta\theta$ (the change in their random kinetic energy), and also to $p\delta(1/\rho)$ (work done by pressure) which tends to expand the volume occupied, i.e.,

$$\delta Q = \delta\theta + p\delta\left(\frac{1}{\rho}\right). \tag{25}$$

Substituting (20), and rearranging, we obtain

$$\frac{\delta Q}{\theta} = \delta \ln\left(\frac{\theta}{\rho}\right). \tag{26}$$

If there is no change in total random energy, i.e. if $\delta Q = 0$, we have

$$\theta = c_\theta \rho \tag{27}$$

and

$$p = c_\theta \rho^2 \tag{28}$$

where c_θ is the ratio θ/ρ, with an initial value, $c_\theta = \theta_0/\rho_0$, which is constant when δQ is zero. Eq. (28) indicates that without any energy input, the random energy of animals will decrease linearly as their abundance decreases. Thus, avoidance events between animals will be reduced when the aggregation is less crowded.

Assuming that animals maintain a constant cruising speed, i.e. $\theta = \theta_0$, we have

$$p = \theta_0 \rho \tag{29}$$

and

$$\Delta Q = \theta_0 \ln\left(\frac{\rho_0}{\rho}\right) \tag{30}$$

where ΔQ is the maximum energy that can be added to maintain the total random energy as abundance changes from its initial value, ρ_0, to some other value, ρ. It is obvious from Eqs. (28) and (29) that, in general, the pressure term is a power function of animal abundance such that

$$p = c_\theta \rho^\beta \tag{31}$$

where β must be greater than 1 and less than 2. Under conditions of local equilibrium, two extreme cases are possible. Either no energy is added to the system ($\beta = 2$), or maximum energy is added to the system ($\beta = 1$). These limits constrain the relationships between abundance, pressure, and random kinetic energy (Fig. 1).

4. An aggregation with uniform, steady mean motion

If an aggregation has no mean motion, or has a uniform steady motion, and the horizontal motion of individuals is much greater than their vertical motion (i.e. $\epsilon = W/U \ll 1$), as occurs in aggregations of Antarctic krill (Hamner *et al.*, 1989) then, based on phenomenological theory (DeGroot and Mazur, 1962), the off-diagonal elements of the pressure tensor e_{ij} are zero because $\partial u_i/\partial x_j = 0$ (see Eq. 19). Thus, we can express the balance between the internal force of autocoherence and the pressure gradient from Eqs. (11) and (24), as follows

$$\frac{1}{\rho}\frac{\partial p}{\partial x} = \int_{-\infty}^{\infty} M\rho(\boldsymbol{\xi})\frac{\partial}{\partial x} G(\boldsymbol{\xi} - \mathbf{x})\, dA_{\boldsymbol{\xi}} \tag{32}$$

$$\frac{1}{\rho}\frac{\partial p}{\partial y} = \int_{-\infty}^{\infty} M\rho(\boldsymbol{\xi})\frac{\partial}{\partial y} G(\boldsymbol{\xi} - \mathbf{x})\, dA_{\boldsymbol{\xi}} \tag{33}$$

$$\epsilon^2\frac{1}{\rho}\frac{\partial p}{\partial z} = \int_{-\infty}^{\infty} M\rho(\boldsymbol{\xi})\frac{\partial}{\partial z} G(\boldsymbol{\xi} - \mathbf{x})\, dA_{\boldsymbol{\xi}} \tag{34}$$

where G is defined by Eq. (23). Substituting relation (31) into the above three equations, and taking the divergence of these equations, we obtain

$$\frac{c_\theta \beta}{\beta - 1}\left\{\frac{\partial^2 \rho^{\beta-1}}{\partial x^2} + \frac{\partial^2 \rho^{\beta-1}}{\partial y^2} + \epsilon^2\frac{\partial^2 \rho^{\beta-1}}{\partial z^2}\right\} = \int_{-\infty}^{\infty} M\rho(\boldsymbol{\xi})\nabla^2 G(\boldsymbol{\xi} - \mathbf{x})\, dA_{\boldsymbol{\xi}}. \tag{35}$$

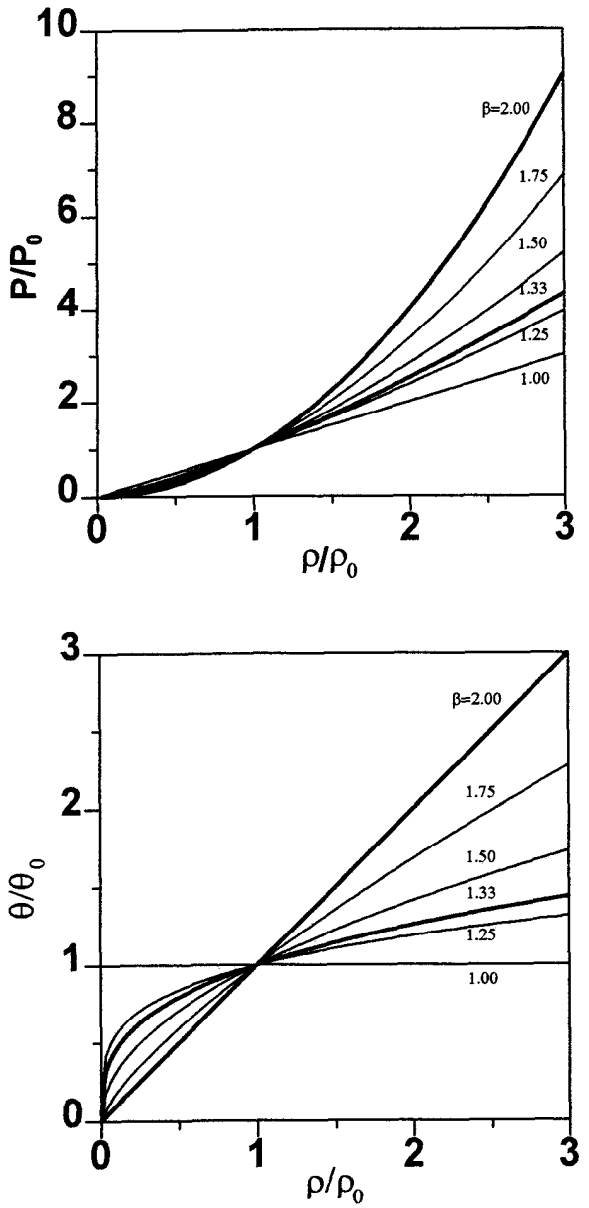

Figure 1. (A) Normalized pressure (p/p_0) and (B) normalized random kinetic energy (θ/θ_0) as a function of normalized abundance (ρ/ρ_0) for hypothetical aggregations in which the power function, β (in Eq. 31), is allowed to vary between its upper and lower limits.

From the formula for G (Eq. 23), it is apparent that G is the three-dimensional Green function for the Poisson equation, and $(1/c_g)\nabla G(\mathbf{x})$ is a δ-function. Thus, Eq. (35) is equal to

$$\frac{c_\theta \beta}{\beta - 1}\left\{\frac{\partial^2 \rho^{\beta-1}}{\partial x^2} + \frac{\partial^2 \rho^{\beta-1}}{\partial y^2} + \epsilon^2 \frac{\partial^2 \rho^{\beta-1}}{\partial z^2}\right\} = M c_g \rho(\mathbf{x}) \tag{36}$$

where c_g, the autocoherence function, can be evaluated from the pressure gradient and the abundance distribution. We refer to c_g, as the "coefficient of biological attraction."

By transforming the coordinates such that

$$x = x', \qquad y = y', \qquad z = \epsilon z' \tag{37}$$

Eq. (36) can then be rewritten as

$$\nabla'^2 \rho^{\beta-1} = \frac{M c_g(\beta - 1)}{c_\theta \beta} \rho(\mathbf{x}') \tag{38}$$

where ∇' is the gradient operator in $\mathbf{x}'$. In this transformed coordinate system, the z direction is streched to the same order of x and y directions, which yields a symmetric solution. Using spheric coordinates, Eq. (38) can be written as the ordinary differential equation

$$\left\{\frac{d^2}{dr^2} + \frac{2}{r}\frac{d}{dr}\right\} \rho^{\beta-1} = \frac{M c_g(\beta - 1)}{c_\theta \beta} \rho(\mathbf{x}') \tag{39}$$

where r is the radial distance in spheric coordinates. Assuming the center of the aggregation is set at the origin of the coordinates, then the abundance (ρ) of animals at any location within the aggregation can be written as

$$\rho = B_0 r^{-m} \tag{40}$$

where both B_0 and m are arbitrary constants which need to be determined. Substituting Eq. (40) into Eq. (39), we obtain

$$B_0^{\beta-1}(\beta - 1) m r^{-m(\beta-1)-2}[(\beta - 1)m - 1] = \frac{M c_g(\beta - 1)}{c_\theta \beta} B_0 r^{-m}. \tag{41}$$

To obtain solutions from Eq. (41), we must have that

$$m = m(\beta - 1) + 2 \tag{42}$$

and

$$B_0^{\beta-1}(\beta - 1) m[(\beta - 1)m - 1] = \frac{M c_g(\beta - 1)}{c_\theta \beta} \cdot B_0. \tag{43}$$

Rearranging Eq. (42), we obtain

$$m = \frac{2}{2 - \beta} \tag{44}$$

where m defines the rate at which animal abundance increases with distance from the edge of the aggregation toward its center.

From the analysis of Eqs. (27) through (30), we demonstrated that the value of β must lie between 1 and 2 (Fig. 1), and therefore it follows from Eq. (44) that $m > 0$. Thus, the abundance of animals will decrease with distance from the center of the aggregation. However, the present solution yields infinite abundance at the origin, which clearly cannot be. To constrain this solution, we assume that there must be some maximum abundance, ρ_{max}, at which the attractive force vanishes, i.e. where the equilibrium distance between animals (r_e) is equivalent to $(1/\rho_{max})^{1/3}$ (Parr, 1927; Breder, 1951; Okubo, 1986). This leads to the solution

$$\rho = \begin{cases} \rho_{max} & \text{where } r \leq a \\ \rho_{max}\left(\dfrac{r}{a}\right)^{-m} & \text{where } r > a \end{cases} \tag{45}$$

where a is that distance from the center of the aggregation at which animal abundance begins to decline from its upper limit, ρ_{max}. Where the abundance is at its maximum ($\rho = \rho_{max}$) then the random kinetic energy also reaches a maximum, $\theta = \theta_{max}$. Rearranging Eq. (31), we obtain

$$c_\theta = \theta_{max}\rho_{max}^{1-\beta} \tag{46}$$

and, substituting Eqs. (44) and (46) into (43), we now solve for the coefficient of biological attraction, c_g

$$c_g = \frac{2\theta_{max}}{M\rho_{max}}(m - 3)(m - 1)a^{-2}. \tag{47}$$

We can now calculate the total number of animals in the aggregation, N, by integrating Eq. (44) over the volume of the aggregation, i.e.

$$N = \int_0^\infty 4\pi r^2 \rho \, dr = \frac{4\pi m}{3(m - 3)} \cdot \rho_{max} a^3 \tag{48}$$

where m must be greater than 3 (there is no solution yielding a finite number of animals in the aggregation when m is equal to or less than 3).

The radius of the aggregation can be defined from the density distribution, i.e.

$$R = \int_0^\infty \rho \, dr \Big/ \rho_{max}. \tag{49}$$

Substituting Eq. (45) into the above definition, we obtain

$$R = \frac{m}{m-1} \cdot a. \tag{50}$$

Eqs. (48) and (50) provide the means to measure the key parameters of animal aggregations. We now have a system of equations that contain a series of measurable variables, namely the maximum abundance of animals near the center of the aggregation (ρ_{max}), the distance from the edge of the aggregation to its center (R), the distance from the center at which the maximal abundance begins to decline (a), the rate of that decline with distance (m), and the total number of animals in the aggregation (N). In practice, all variables are measurable, and lead to a value for the coefficient of biological attraction.

5. The biological force of attraction, and its role in maintaining aggregations

We can now evaluate the constant of animal attraction, c_g, as a function of measurable variables. Combining (47) and (50), and cancelling a, we obtain

$$c_g = \frac{2\theta_{max}}{M\rho_{max}} \frac{(m-3)m^2}{(m-1)R^2}. \tag{51}$$

The dimensions of the autocoherence function are

$$[c_g] = \frac{[\mathrm{m^2\ s^{-2}}]}{[\mathrm{kg\ m^{-3}}]} [\mathrm{m^{-2}}] = [\mathrm{N \cdot m^2 \cdot kg^{-2}}] \tag{52}$$

which is dimensionally equivalent to Newton's gravitational constant. Thus, c_g is the biological attraction. The force of attraction, F_A, between two animals of masses M_1 and M_2 is described by

$$F_A = \frac{c_g(M_1 \cdot M_2)}{d^2} \tag{53}$$

where d is the distance between them.

Although the highest swimming speeds, or "escape velocities," can be maintained for very brief periods, marine animals tend to swim at a constant velocity, or "cruising speed" (Zhong *et al.*, 1996). The maximum kinetic energy of animals in an aggregation, θ_{max}, is therefore well represented as a function of the cruising speed. Rearranging (51), we obtain

$$\theta_{max} = \frac{p_{max}}{\rho_{max}} = \frac{M\rho_{max}c_gR^2(m-1)}{2(m-3)m^2} \tag{54}$$

which represents the bulk balance of forces in the aggregation. The potential stored in the pressure field causes the aggregation to expand, and the autocoherent force of attraction causes it to contract.

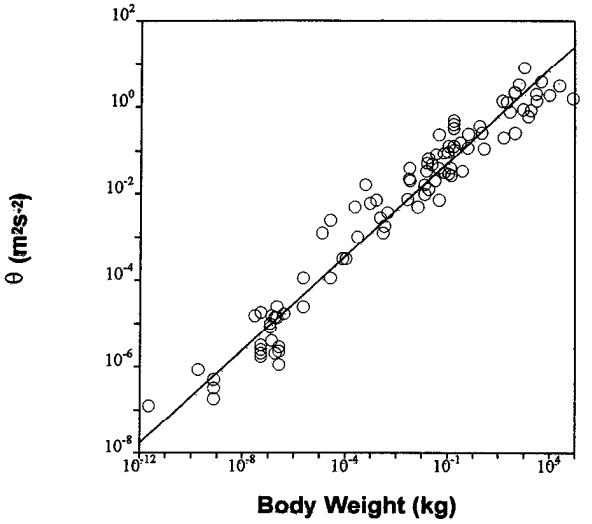

Figure 2. Random kinetic energy ($m^2\ s^{-2}$) as a function of body wet mass (kg) for marine animals ranging in size from protozoans to whales. Data from Zhong *et al.* (1996).

Kinetic energy is a function of animal mass (Fig. 2; Zhong *et al.*, 1996). Thus, Eq. (54) is appropriately scaled by rearranging as

$$\theta_{max} = R \cdot \phi(M) \tag{55}$$

where the normalized force of attraction, $\phi(M)$, is

$$\phi(M) = \frac{M\rho_{max}c_g R(m-1)}{2(m-3)m^2} \tag{56}$$

represents the force exerted by the mass of all animals in the aggregation on a unit mass of individual. Figure 3 shows that, for a given magnitude of attractive force, large animals can maintain larger aggregations than small animals.

6. Observations of the autocoherent force, F_I, in an aggregation of Antarctic krill

a. Methods. Application of the bio-continuum theory is limited only by the measurability of its defined variables. Here we provide an example using measurements on aggregations of Antarctic krill (*Euphausia superba*). Acoustic Doppler technology offers the instrument of choice for this task, as it is capable of providing the necessary *in situ* measurements of distribution and abundance.

In July 1992, euphausiids were the primary Doppler scatterers in Gerlache Strait, Antarctica. Data collected by Acoustic Doppler Current Profiler (ADCP) during the RACER IV 1992 winter expedition (Zhou *et al.*, 1994) can be used to measure the key

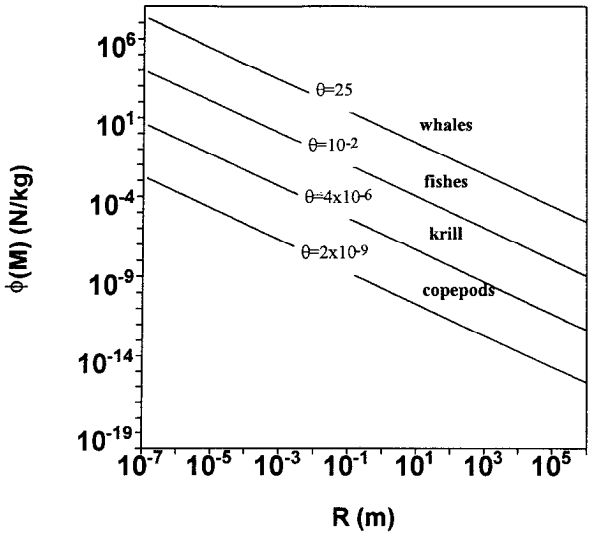

Figure 3. The mass-normalized force of attraction (N kg^{-1}), calculated from Eq. (56) as a function of the radius of the animal aggregation (m) for characteristic individual mass of representative marine animals: copepods, krill, fishes and whales.

variables required to characterize krill aggregations according to the bio-continuum theory, and from these to estimate the coefficient of biological attraction for *Euphausia superba.*

In the Gerlache and Bransfield Straits, circulation in the upper layer has scales of 10^4 to 10^5 meters (Niiler *et al.,* 1991; Huntley and Niiler, 1995). This circulation scale is one order of magnitude greater than the scale of krill aggregations (10^1 to 10^3 m). Thus, the assumption that patches are drifting in the uniform mean flow fields, and are in a quasi-steady state with respect to external physical forcing, is justified.

A hull-mounted 153 kHz ADCP (RD Instruments, San Diego, CA) was set to collect data using a bin width of 4 m, a pulse length of 4 m, and a ping interval of 4 s. The wavelength of sound at 153 kHz is approximately equal to 1 cm at a sound speed of 1474 m s^{-1} in Antarctic waters of typical temperature (1°C) and salinity (34‰), constraining the size of organism that can be detected. From such theoretical considerations, as well from the analysis of samples collected by MOCNESS, Zhou *et al.* (1994) demonstrated that their measurements of echo intensity represented the total volume or biomass of three species of euphausiids, *Euphausia superba, E. crystallorophias* and *Thysanoessa macrura.* The euphausiid biomass was overwhelmingly dominated by *E. superba* of 21–24 mm in length. Taking the average length of euphausiids at 22 mm, and the individual target strength at −79 dB, biomass and abundance were directly measured from ADCP data.

b. Results. Here we demonstrate the application of theory to a krill aggregation with scales of 150 m in the vertical and 2 km in the horizontal, and centered at 120 m depth (Fig. 4). The abundance at its center was approximately 8 animals m^{-3}. The aggregation was

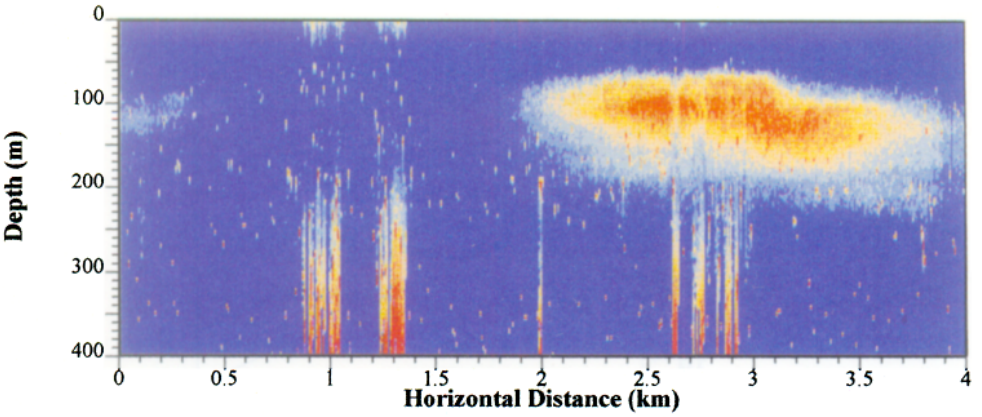

Figure 4. Antarctic krill, *Euphausia superba:* Echo observations from ADCP relative to depth (m) and distance (km) in Gerlache Strait, Antarctic Peninsula in July, 1992.

discrete, having sharp edges. A horizontal section through the abundance maximum at 120 m reveals that abundance increased monotonically toward the center of the aggregation, and then was approximately constant (i.e. $\rho = \rho_{max} = 8$) for a distance of almost one km (Fig. 5). This feature is made clearer when the log-transformed abundance is plotted against distance, normalized to the x-dimension of the aggregation (Fig. 6; $L = 1.2$ km). This observation supports our solution of Eq. (45), i.e. that abundance may attain a constant value near the center of an aggregation. The circles in Figure 6 are observations of the right side of the aggregation; and diamonds are those of the left side. The two solid lines are the low-pass data obtained after filtering the high frequency noise. The transition from ρ_{max} to lower abundance occurs where the slope is broken, at $r/L = 0.4$, which from Eq. (45) leads to $a = 500$ m. It is clear that the gradient of abundance at $\rho = \rho_{max}$ is gradual rather than abrupt. Above the transient region, the slope, m, attained a value of 8, which is a possible steady state solution for the condition of $m > 3$, as implied by Eq. (48). From Eq.

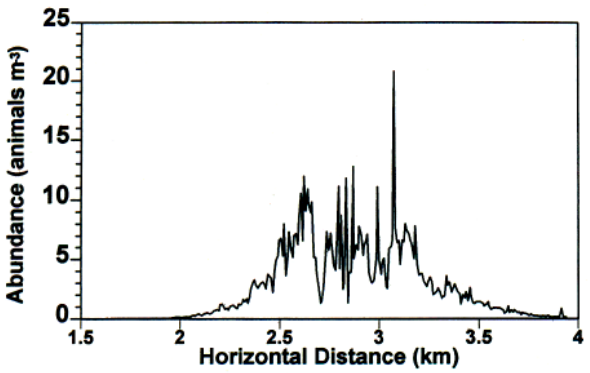

Figure 5. *Euphausia superba:* Abundance (individuals m^{-3}) along a horizontal transect at 120 m depth through the aggregation shown in Figure 4.

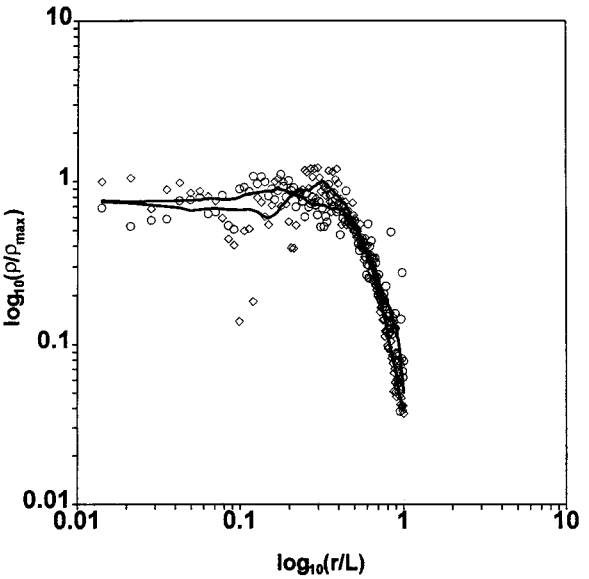

Figure 6. *Euphausia superba:* Normalized abundance (ρ/ρ_{max}) as a function of normalized distance (r/L) through the aggregation shown in Figure 4. Circles represent data to the right of the patch center; diamonds are on the left of center. Dark lines are the low-pass filtered data.

(50), we calculate $R = 570$ m, recalling that R is defined as the mean radius of the abundance distribution function (Eq. 49).

The constant of animal attraction, c_g, can be estimated for this aggregation as follows. First, we made no direct measurements of swimming velocity, so we estimate the random kinetic energy using Zhong *et al.*'s (1996) relation (Fig. 3)

$$\theta = 0.117M^{0.43} \tag{57}$$

where M is the mass, in wet weight (kg). For *Euphausia superba* of 22 mm body length, $M = 1 \times 10^{-4}$ kg, which yields $\theta = 2.23 \times 10^{-3}$ kg m^2 s^{-2}. Applying Eq. (51), the constant of biological attraction for the aggregation (Fig. 4) is

$$c_g = 7.8 \times 10^{-4} \qquad \text{N m}^2\,\text{kg}^{-2}. \tag{58}$$

This suggests, applying Eq. (53), that two *Euphausia superba* separated by 1 m within this aggregation would experience an attractive force equivalent to 7.8×10^{-12} N.

7. Universality of the force of animal attraction

The phenomenon of attraction has been widely observed among animals. A large number of insects and other terrestrial animals are known to emit and respond to chemical gradients, perhaps the most famous example being that of the silk moth, *Bombyx mori,* which produces a remarkably powerful compound (bombykol) that acts as a sex attractant

over great distances. Some marine organisms may also use chemical signals to "communicate" with one another, although the usefulness of this mechanism is limited to small scales because of the significantly lower rates of molecular diffusion in water by comparison to air. Marine animals with highly evolved visual systems, such as fishes, may rely upon images to recognize members of their own species, whereas those with less evolved visual apparatus, such as copepods and euphausiids, may rely upon bioluminescent emissions at species-specific wavelengths to accomplish the same function. Marine mammals employ yet another means, acoustics, to communicate with one another. In summary, much is known about the physiological mechanisms of animal communication.

Aggregation of species into highly compact groups is also a well-recognized phenomenon and one in which the mechanisms of attraction, alluded to above, must certainly play a role. The occurrence of pods of mammals, schools of fishes, swarms of euphausiids, and patches of copepods suggests that such aggregations are a common feature of species-specific organization at an ecological level below that of the population.

The bio-continuum theory presented here is aimed at elucidating the fundamental principles that underlie the dynamics of animal aggregations. We have sought to define, in a formal manner, the force of biological attraction that causes the observed spatial autocoherence of species at the appropriate scales. This is done without reference to the detailed physiological mechanisms that are proximally responsible for the formation and maintenance of pods, schools or swarms; we assume that these mechanisms are scaled in a manner that allows their effects to be reduced to simple mathematical statements that transcend species differences.

The "coefficient of biological attraction" we have defined can clearly be evaluated for *Euphausia superba.* Is it a "constant of biological attraction," and therefore a universal value? We cannot say. To explore the possibility that c_g is constant will require observations of the aggregations of species of different mass and taxonomic origin, with very careful measurements of the key parameters of the theory presented here. The required measurements, given by Eq. (51), are the random kinetic energy (θ), the mass of an individual animal (M), its maximum abundance in the aggregation (ρ_{max}), the size of the aggregation (R), and the rate at which abundance decreases near the edge of the aggregation (m). We note that the random kinetic energy can be directly estimated from measurements of swimming velocity, and that the estimate of c_g is particularly sensitive to the value for m.

For observations of micronekton and nekton, acoustic Doppler technology may prove especially applicable, as this methodology allows direct measurement of most of the necessary variables. From the Doppler spectrum, the mean Doppler shift represents the mean motion of back scatterers with the relation

$$V_D = C\frac{F_D}{2F_S} \tag{59}$$

where V_D is the relative velocity between the sound source and the sound receiver, C is the speed of sound, F_D is the Doppler shift, and F_S is the acoustic system frequency. In an

aggregation of micronekton or nekton, the random motion of swimming patterns causes a broadening of the Doppler spectrum, from which the mean motion is directly calculated. The resultant spectral broadening exactly represents the velocity distribution of animals in the ensonified volume along the transducer (Holliday, 1974, 1977), from which both the mean motion ($\mathbf{u}$) and the random kinetic energy (θ) can be measured. Application of the ADCP allows direct measurement of other necessary variables (R, m, and ρ_{max}), as demonstrated elsewhere (Figs. 4–6 and Zhou *et al.,* 1994). Individual mass, M, can be measured by collecting animals in nets and weighing them following standard techniques. Measurements of aggregation parameters on large fishes and mammals might also be accomplished by acoustic techniques, using lower frequencies than for nekton, but we expect that observations of very large mammals may prove especially challenging and would require other methods.

To discover that the coefficient of biological attraction is constant would obviously lead to a better understanding of the principles that govern conspecific association. While one anticipates the arrival of data that address this hypothesis, it is interesting to ponder that, at least for *Euphausia superba,* the coefficient of biological attraction (7.8×10^{-4} N m^2 kg^{-2}) is approximately 7 orders of magnitude greater than the constant of gravitational attraction (6.670×10^{-11} N m^2 kg^{-2}).

Acknowledgments. We thank D. V. Holliday for discussing issues regarding the application of acoustic Doppler techniques, and S. Beaulieu, A. Gonzalez, M. Lopez, W. Nordhausen, V. Øresland, and P. J. Perl for helping to collect field data. Special thanks are due to RD Instruments (San Diego, California) and, in particular, to Michael Metcalf and Darrell Simons. We thank two anonymous reviewers, and specifically E. Hofmann, for comments which improved the final manuscript. Theoretical aspects of this research were supported by Office of Naval Research grant number N00014-92J-1618 to M. Huntley and NSF grant number OPP95-2374B to M. Huntley and M. Zhou. Field research was supported by grant number DPP-88-17779 from the Office of Polar Programs, National Science Foundation, also to M. Huntley. This is contribution no. 8 of the Simon J. Poole Institute.

REFERENCES

Anderson, J. J. 1981. A stochastic model for the size of fish schools. Fish. Bull. U.S., *19,* 315–323.

Antezana, T. and K. Ray. 1983. Aggregation of *Euphausia superba* as an adaptive group strategy to the Antarctic ecosystem. Ber. Polarforsch., *4,* 199–215.

Baars, M. A. and S. S. Oosterhuis. 1985. Zooplankton grazing in natural water with high concentration of ^{14}C bicarbonate: variable live controls and gut passage time. Hydrobiol. Bull. *19,* 71–80.

Blaxter, J. H. S. 1969. Swimming Speeds of Fish. FAO Fish. Rep., *62,* 69–100.

Bollens, S. M., B. W. Frost and J. R. Cordel. 1994. Chemical, mechanical and visual cues in the vertical migration behavior of the marine planktonic copepod *Acartia hudsonica.* J. Plankton Res., *16,* 555–564.

Breder, C. M. 1951. Studies on the structure of the fish school. Bull. Amer. Mus. Nat. Hist., *98,* 1.

Brock, V. E. and R. H. Riffenburgh. 1960. Fish schooling: A possible factor in reducing predation. J. Cons. Int. Perm. Explor. Mer, *25,* 307–317.

Buskey, E. J. and D. K. Stoecker. 1989. Behavioral responses of the marine tintinnid *Favella* sp. to phytoplankton: Influence of chemical, mechanical and photic stimuli. J. Exp. Mar. Biol. Ecol., *132,* 1–16.

Clark, C. W. 1974. Possible Effects of Schooling on the Dynamics of Exploited Fish Populations. Wiley-Interscience, NY, 322 pp.

Cowles, T. J., R. A. Desiderio and S. Neuer. 1993. *In situ* characterization of phytoplankton from vertical profiles of fluorescence emission spectra. Mar. Biol., *115,* 217–222.

Dagg, M. J. 1985. The effects of food limitation on diel migratory behavior in marine zooplankton. Arch. Hydrobiol. Beih. Ergebn. Limnol., *21,* 247–255.

Dam, H. G. and W. T. Peterson. 1993. Seasonal contrasts in the diel vertical distribution, feeding behavior, and grazing impact of the copepod, *Temora longicornis* in Long Island Sound. J. Mar. Res., *51,* 561–594.

DeGroot, S. R. and P. Mazur. 1962. Non-equilibrium Thermodynamics. North-Holland Publishing Company, Amsterdam, 456 pp.

Duffy, D. C. and C. Wissel. 1988. Models of fish school size in relation to environmental productivity. Ecol. Mod., *40,* 201–211.

Duval, W. S. and G. H. Geen. 1976. Diel feeding and respiration rhythms in zooplankton. Limnol. Oceanogr., *21,* 823–829.

Flagg, C. N. and S. L. Smith. 1989. On the use of the acoustic Doppler current profiler to measure zooplankton abundance. Deep-Sea Res., *36,* 455–474.

Hamner, P. and W. M. Hamner. 1977. Chemosensory tracking of scent trails by the planktonic shrimp *Acetes sibogae australis.* Science, *195,* 886–888.

Hamner, W. M. 1984. Aspects of schooling in *Euphausia superba.* J. Crust. Biol., 4 (Spec. No. 1), 67–74.

Hamner, W. M., P. P. Hamner, B. S. Obst and J. H. Carleton. 1989. Field observations on the ontogeny of schooling of *Euphausia superba furciliae* and its relationship to ice in Antarctic waters. Limnol. Oceanogr., *34,* 451–456.

Hamner, W. H., P. P. Hamner, S. W. Strand and R. W. Gilmer. 1983. Behavior of Antarctic krill, *Euphausia superba:* chemoreception, feeding, schooling and moulting. Science, *220,* 433–435.

Head, E. J. H., R. Wang and R. J. Conover. 1984. Comparison of diurnal feeding rhythms in *Temora longicornis* and *Centropages hamatus* with digestive enzyme activity. J. Plankton Res., *6,* 543–551.

Holliday, D. V. 1974. Doppler structure in echoes from schools of pelagic fish. J. Acoust. Soc. Am., *55,* 1313–1322.

—— 1977. Two applications of the Doppler effect in the study of fish schools. Rapp. P.-v. Cons. Int. Perm. Explor. Mer, *170,* 21–30.

Horn, H. S. 1968. The adaptive significance of colonial nesting in Brewer's blackbird (*Euphagus cyanocephalus*). Ecology, *49,* 682–694.

Horwood, J. W. and D. H. Cushing. 1978. Spatial distributions and ecology of pelagic fish, *in* Spatial Pattern in Plankton Communities, J. H. Steele, ed., Plenum Press, NY, 355–383.

Huntley, M. E. and E. R. Brooks. 1982. Effects of age and food availability on diel vertical migration of *Calanus pacificus.* Mar. Biol., *71,* 23–31.

Huntley, M. E. and P. P. Niiler. 1995. Physical control of population dynamics in the Southern Ocean. ICES J. Mar. Sci., *52,* 457–468.

Huntley, M. E., W. Nordhausen and M. D. G. Lopez. 1994. Elemental composition, metabolic activity and growth of Antarctic krill, *Euphausia superba* Dana, during winter. Mar. Ecol. Prog. Ser., *107,* 23–40.

MacArthur, R. H. and E. R. Pianka. 1966. On the optimal use of a patchy environment. Am. Nat. *100,* 603–609.

Mayzaud, O., P. Mayzaud, C. de la Bigne and P. Grohan. 1984. Diel changes in the particulate environment, feeding activity and digestive enzyme concentration in neritic zooplankton. J. Exp. Mar. Biol. Ecol., *84,* 15–35.

Niiler, P. P., A. Amos and J.-H. Hu. 1991. Water masses and 200 m relative geostrophic circulation in the western Bransfield Strait region. Deep-Sea Res., *38,* 943–960.

Okubo, A. 1980. Diffusion and ecological problems: Mathematical Models, Biomathematics. Springer-Verlag, Berlin, 254 pp.

—— 1986. Dynamical aspects of animal swarming: swarms, schools, flocks and herds. Adv. Biophys., *22,* 1–94.

Okubo, A. and J. J. Anderson. 1984. Mathematical models for zooplankton swarms: their formation and maintenance. EOS, *65,* 731–732.

Parr, A. E. 1927. A contribution to the theoretical analysis of the schooling behavior of fishes. Occas. Pap., Bingham Oceanogr. Coll., 32.

Partridge, B. L. 1982. The structure and function of fish schools. Am. Sci., *246,* 90–99.

Pitcher, T. J. 1983. Heuristic definitions of fish shoaling behavior. An. Behav., *31,* 611–613.

Poulet, S. A. and G. Ouellet. 1982. The role of amino acids in chemosensory swarming and feeding of marine copepods. J. Plankton Res., *4,* 341–361.

Pyke, G. H., H. R. Pulliam and E. L. Charnov. 1977. Optimal foraging: a selective review of theory and tests. Wart. Rev. Biol., *52,* 137–154.

Radakov, D. V. 1973. Schooling in the Ecology of Fish, Halstead-John Wiley, NY, Israel Program for Scientific Translations.

RDI. 1989. Acoustic Doppler Current Profilers. Principles of Operation: A Practical Primer. RD Instruments, San Diego, 36 pp.

Saiz E., P. Tiselius, P. R. Jonsson, P. Verity and G.-A. Paffenhöfer. 1993. Experimental records of the effects of food patchiness and predation on egg production or *Acartia tonsa.* Limnol. Oceanogr., *38,* 280–289.

Shaw, E. 1978. Schooling Fishes. Am. Sci., *66,* 166–175.

Smith, S. L., R. E. Pieper, M. V. Moore, L. G. Rudstam, C. H. Greene, J. E. Zamon, C. N. Flagg and C. E. Williamson. 1992. Acoustic techniques for the *in situ* observation of zooplankton. Arch. Hydrobiol. Beih. Ergebn. Limnol., *36,* 23–43.

Steele, J. H. and E. W. Henderson. 1992. A simple model for plankton patchiness. J. Plank. Res., *14,* 1397–1403.

Steele, J. H. and M. M. Mullin. 1977. Zooplankton dynamics, *in* The Sea, E. D. Goldberg, ed., *6,* Wiley-Interscience, NY, 857–890.

Stretch, J. J., P. P. Hamner, W. M. Hamner, W. C. Michel, J. Cook and C. W. Sullivan. 1988. Foraging behavior of antarctic krill *Euphausia superba* on sea ice microalgae. Mar. Ecol. Prog. Ser., *44,* 131–139.

Swartzmann, G. 1991. Fish school formation and maintenance: a random encounter model. Ecol. Mod., *56,* 63–80.

Test, F. H. and R. G. McCann. 1976. Foraging behavior of *Bufo americanus* in response to high densities of micro-organisms. Copeia, *3,* 576–578.

Zhong, X., M. E. Huntley and M. Zhou. 1996. The influence of animals on turbulence in the sea. EOS, *76* (Suppl.), 150.

Zhou, M., W. Nordhausen and M. E. Huntley. 1994. ADCP measurements of the distribution and abundance of euphausiids near the Antarctic Peninsula in winter. Deep-Sea Res., *41,* 1425–1445.

Received: *25 April, 1995;* revised: *14 May, 1996.*